

Supporting Information

Chemical Vapor Deposition Grown Formamidinium Perovskite Solar Modules with High Steady State Power and Thermal Stability

Matthew R. Leydent[†], Yan Jiang[†], Yabing Qi^{*, †}

[†] *Energy Materials and Surface Sciences Unit (EMSS), Okinawa Institute of Science and Technology Graduate University (OIST), 1919-1 Tancha Onna-son, Okinawa 904-0495 Japan.*

**Corresponding Author E-mail: Yabing.Qi@OIST.jp*

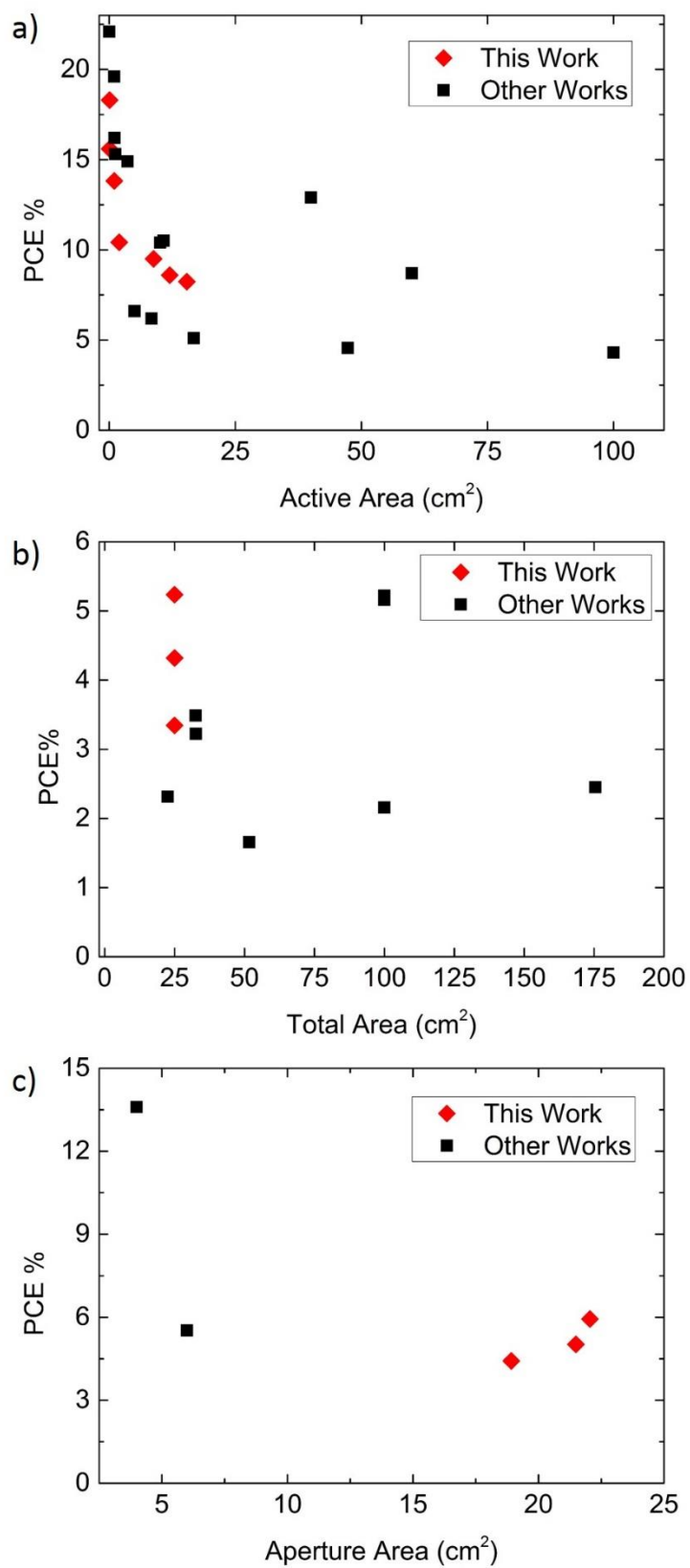


Fig. S1 Reported module efficiency as a function of area measured by *J-V* curve, presented in terms of a) PCE per active area, b) PCE per total area, and c) PCE per aperture area. In all three cases, PCEs show a steep drop off as area is increased.

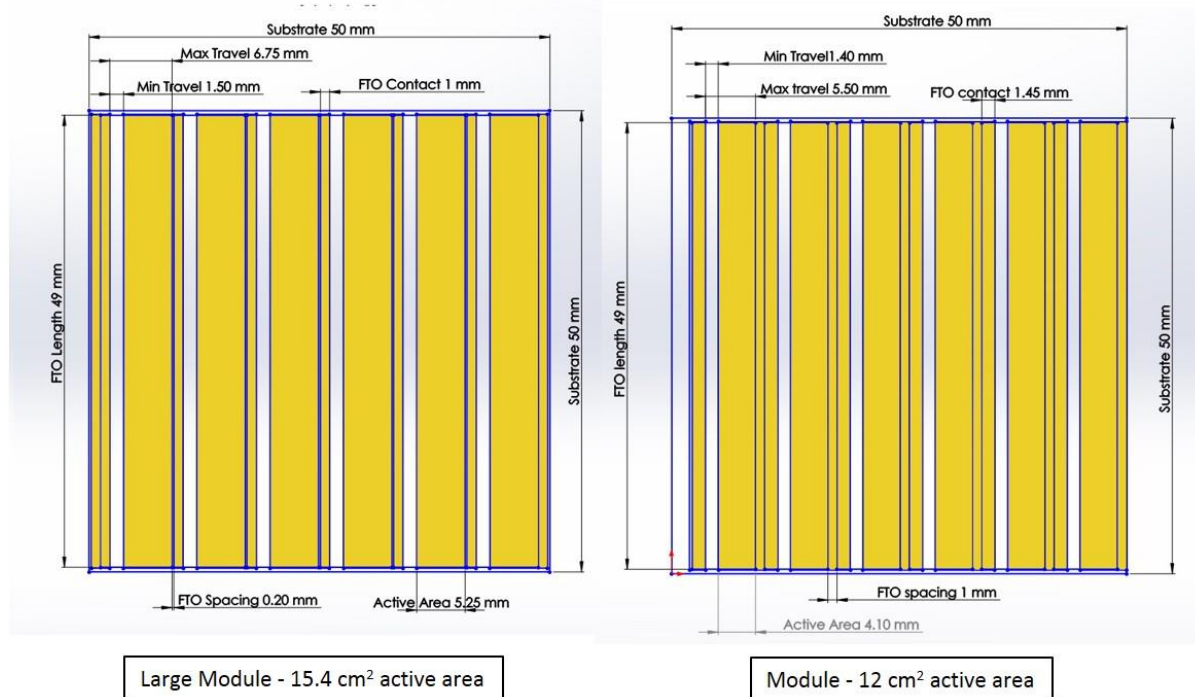
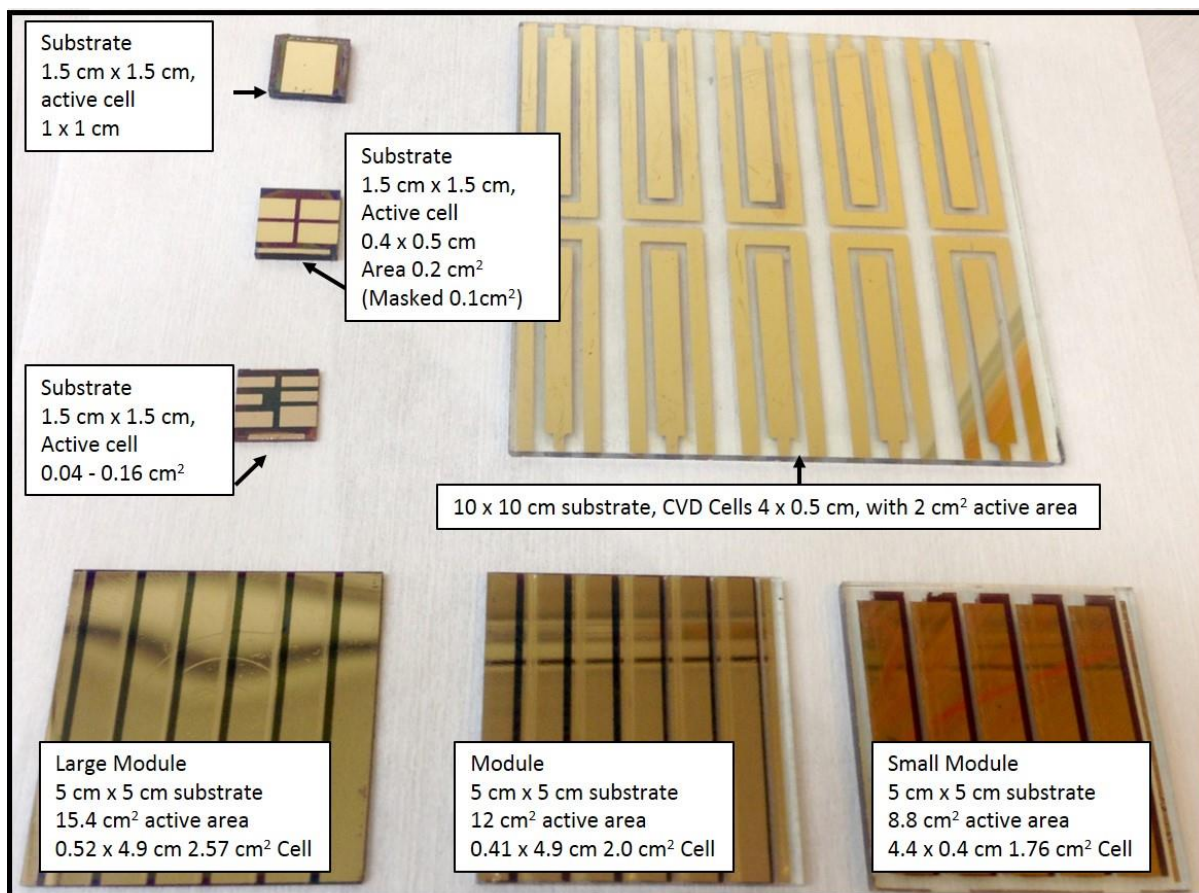


Fig. S2 Geometry of modules and cells presented in this work.

The series resistance of each cell can be measured from the slope of line at V_{oc} (positive to negative scan). The average series resistance of the individual cells was found to be 11Ω for the small module 8.8 cm^2 , and 12Ω for both the 12 cm^2 module, and 15.4 cm^2 module. For the 12 cm^2 module the average travel distance through FTO is $\sim 3.5 \text{ mm}$, for an average aspect ratio of ~ 2.9 , and we would then expect a series resistance of approximately $2.8 \Omega/\text{cm}$ for $8 \Omega/\text{square FTO}$, or 13.5Ω for a 49 mm long cell.

We can estimate the impact of series resistance by considering an idealized cell with J_{sc} of $20 \text{ mA}/\text{cm}^2$, V_{oc} of 1 V , and series resistance of 13.5Ω . This cell would have a maximum power point at 0.5 V and a PCE of 9.2% . This is in good agreement with the PCE of 8.8% for the 12 cm^2 module, but had a different maximum power point $0.68 \text{ V}/\text{cell}$. In order for this model cell to have the same PCE as the champion small area cell of 15.6% the cell needs to have a low series resistance of $1.2 \Omega/\text{cm}$, which corresponds to a relatively narrow cell with an average travel distance of $\sim 1.5 \text{ mm}$.

The series resistance of the whole 6 cell modules was measured by positive to negative scan to be $\sim 40 \Omega$, and for negative to positive scan $\sim 50 \Omega$. This is lower than the sum of all individual cells $\sim 6\text{-}8 \Omega/\text{cell}$. This is possibly due to capacitive like hysteresis effects that make it appear that the series resistance is lower what would be measured in steady state.

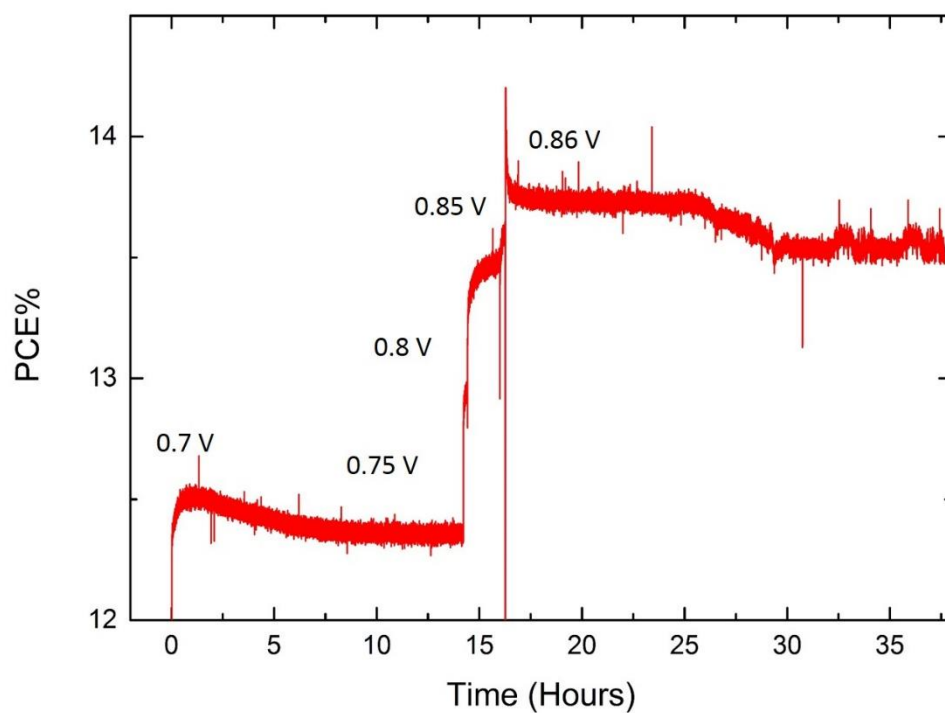


Fig. S3 Steady state power measurement of champion 1 cm^2 solution processed cell. After 14 hours of measurement the maximum power point is manually adjusted to 0.86 V.

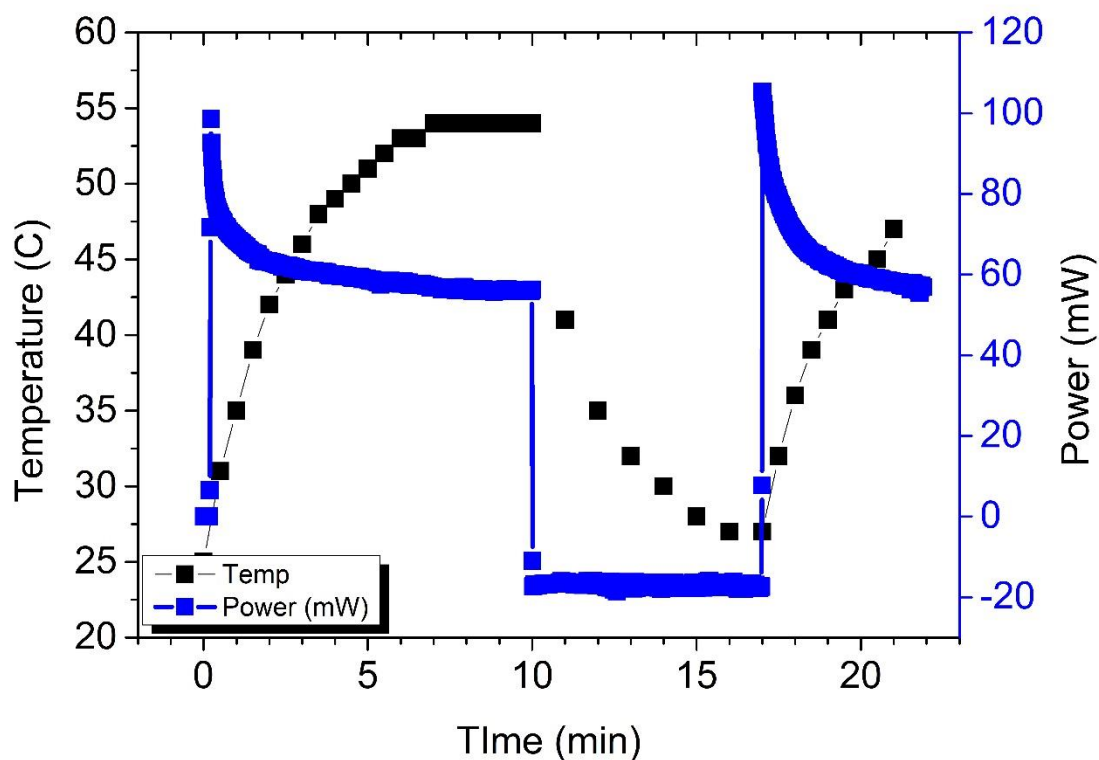


Fig S4 Temperature dependence of MAI based solution processed module operated at the approximate maximum power point (3.9 V) under 1 Sun, which clearly shows that higher temperatures correlated to lower steady state current. The power of the module returned when the cell was allowed to cool. Note that this module had significant dark current after heating, causing a negative power reading of approximately 20 mW (4.3 mA) when the light is turn off. This dark current was a function of heating time and temperature, and time in the cool state.

For example this module was measured many times over 2 days, and the dark current at 3.9 V was recorded before and after heating 3 times:

Measurement 1 (Time 0 h: dark current 0.01 mA, Heated 10 min to 53 °C: dark current 4.3 mA).

Measurement 2 (Time 30 h: dark current 2.4 mA, Heated 15 min to 53 °C: dark current 5.2 mA)

Measurement 3 (Time 31 h: dark current 3.9 mA, Heated 15 min to 63 °C: dark current 8.3 mA)

From this data it is clear to see that the dark current is a function of heating history, and will partially recover to low values given enough time.

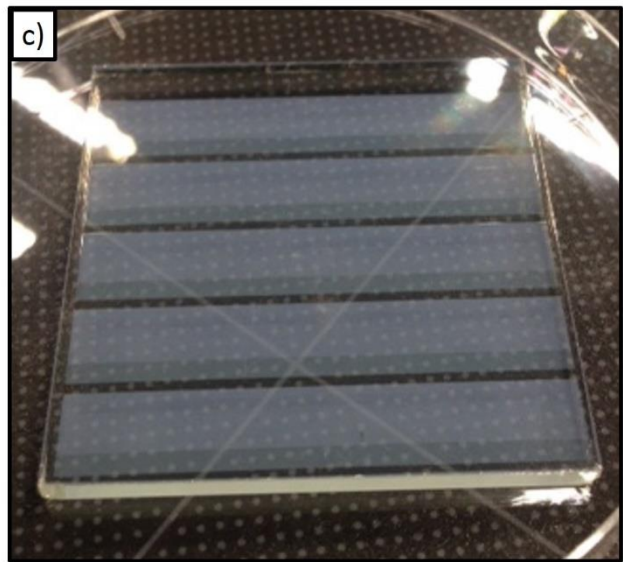
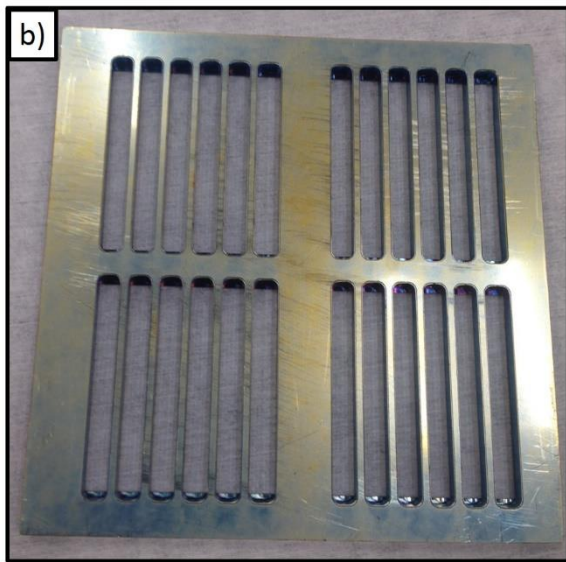
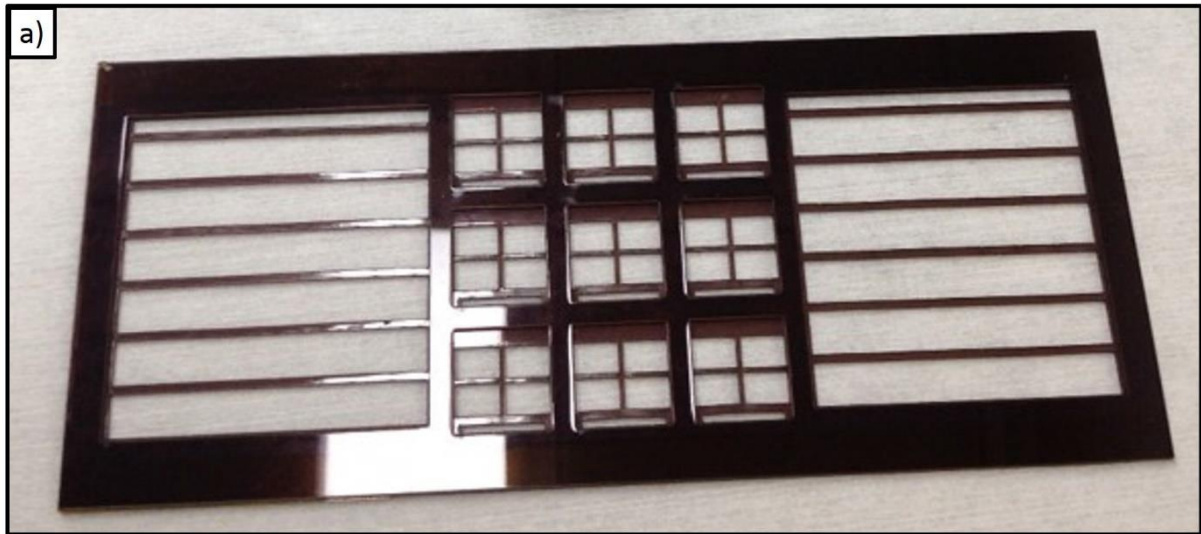


Fig. S5 Patterning by use of mask or photolithography. a) Shadow mask used for patterning gold electrodes for the large module (15.4 cm²). b) Steel mask used for patterning the TiO₂ layer of the 12 cm² modules. c) Dry etching of TiO₂ by inductively coupled plasma. Contrast between TiO₂ coated FTO and FTO where the TiO₂ has been removed is visible in this photograph.

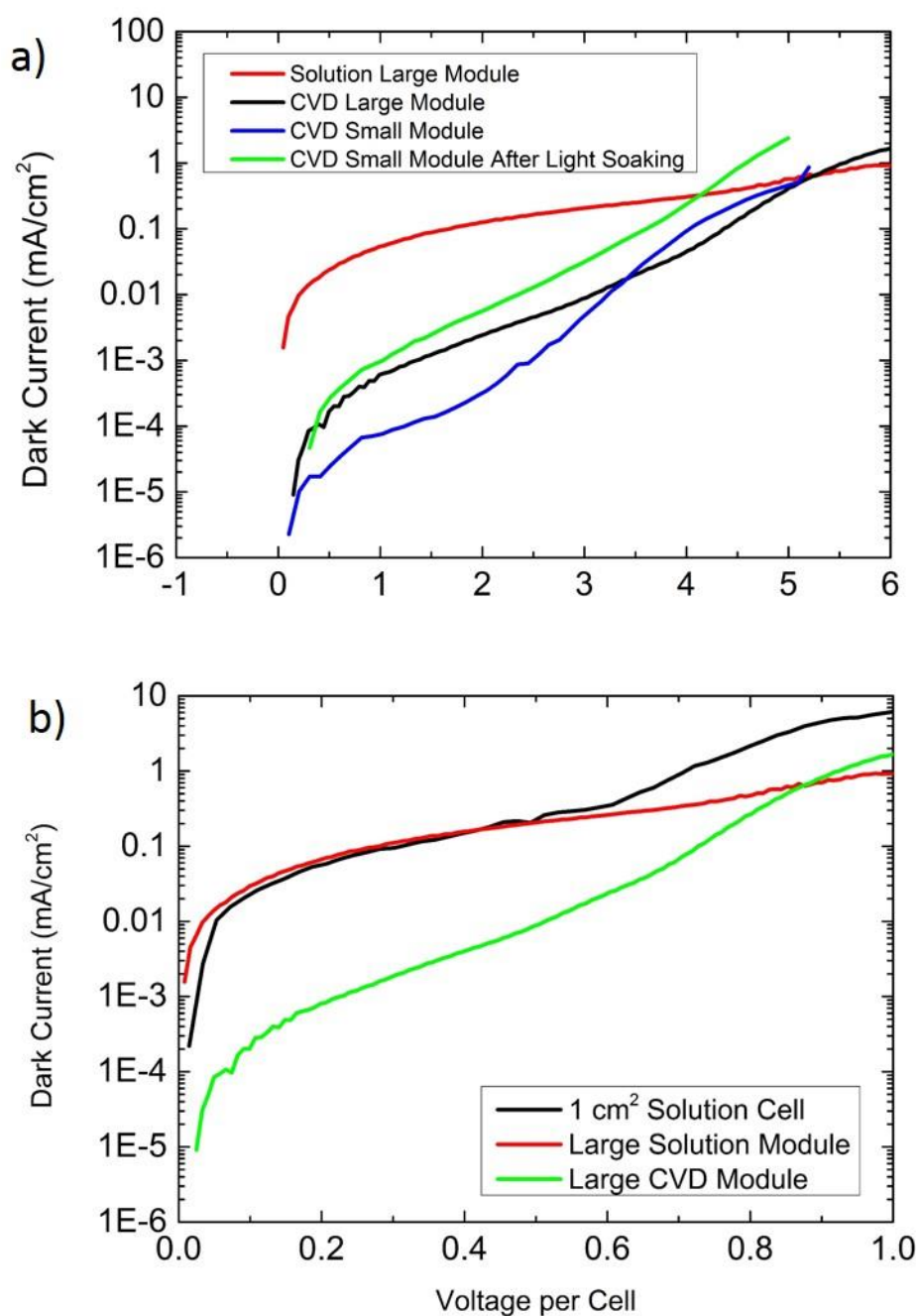


Fig. S6 Dark Current density measurements on solution and CVD processed modules. These measurements reveal that the dark current showed a higher magnitude on the solution modules than the CVD modules. We showed in Figures 3 and S3 that dark current is related to cell heating, and differences between MAI and FAI based perovskite. However differences could also be due to the TiO₂ formation process, which differs in the two processes. If we scale the voltage per cell and measure the dark current of a smaller single cell we see analogous behaviour. This indicates that the high dark current is not related to the module processing but rather some steps that are common to all solution processed cells., e.g. possibly the mesoporous TiO₂ is not as effective a blocking layer as the compact layer prepared by spray pyrolysis.

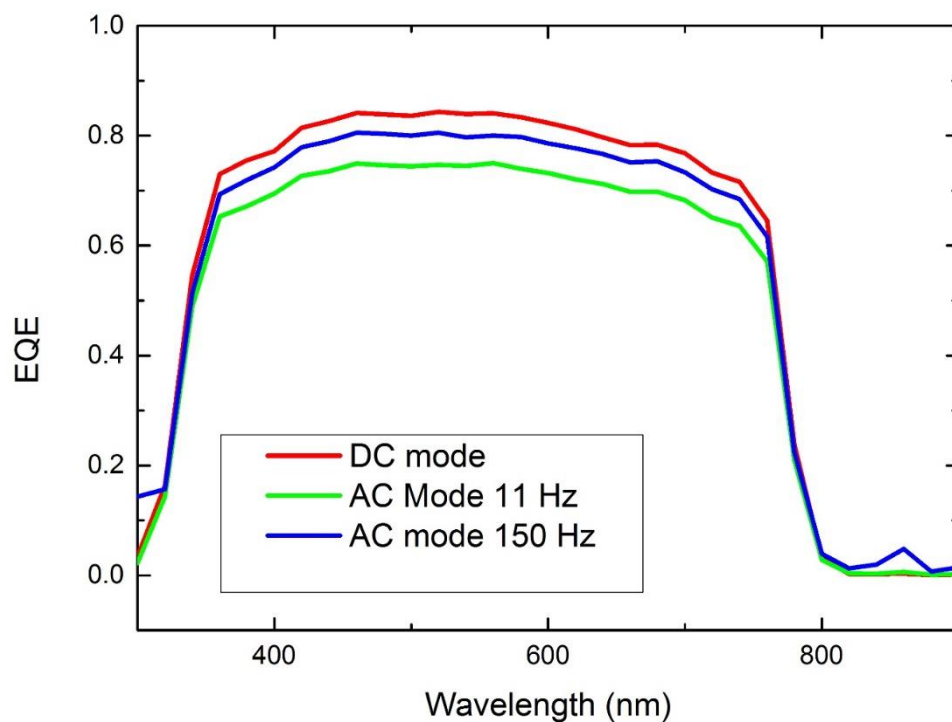


Fig. S7 External Quantum Efficiency (EQE) of a solution processed cell measured in different modes. The J_{sc} measured by solar simulator for this cell was 21.7 mA/cm^2 . This is in reasonable agreement with the integrated current from the DC EQE measurement of 20.3 mA/cm^2 . The AC mode was found to work reasonably well if the frequency was relatively high, 150 Hz, and gave an integrated current of 19.5 mA/cm^2 . When the frequency was at the lowest setting, 11 Hz, the integrated current was in poorer agreement, 18.1 mA/cm^2 .